BMC Cancer

RESEARCH

Open Access

ADORA2B promotes proliferation and migration in head and neck squamous cell carcinoma and is associated with immune infiltration

Pian Li[1†], Ke-ling Pang[2†], Shuang-jing Chen[3], Dong Yang[1], Ai-tao Nai[1], Gui-cheng He[1], Zhe Fang[1], Qiao Yang[1], Man-bo Cai[1*] and Jun-yan He[1*]

Abstract

Background Adenosine A2B receptor (ADORA2B), a G protein-coupled receptor, is implicated in tumor progression and immune regulation in various cancers. However, its specific role in head and neck squamous cell carcinoma (HNSC) remains largely unexplored. This study aims to elucidate the expression profile, prognostic value, immune modulatory role, and therapeutic potential of ADORA2B in HNSC.

Methods Comprehensive bioinformatics analyses were performed using TCGA and GEO datasets to evaluate ADORA2B expression, clinical correlations, and prognostic significance in HNSC. Weighted gene co-expression network analysis (WGCNA) and functional enrichment analyses were conducted to explore ADORA2B-associated pathways. Immune infiltration was assessed via ESTIMATE and single-sample gene set enrichment analysis (ssGSEA). Immune checkpoint blockade (ICB) therapy sensitivity and drug sensitivity were analyzed using the IMvigor210 and NCI-60 databases, respectively. In vitro experiments, including siRNA-mediated ADORA2B knockdown, CCK-8 assays, colony formation, and wound healing assays, were performed to validate the oncogenic role of ADORA2B.

Results ADORA2B was significantly overexpressed in HNSC tumor tissues compared to adjacent normal tissues, and its expression correlated with advanced clinical stage as well as poor overall survival (OS) and progression-free survival (PFS). Functional enrichment analyses revealed significant downregulation of immune-related pathways in high ADORA2B expression groups. High ADORA2B expression was associated with a more immunosuppressive tumor microenvironment (TME), characterized by lower immune and stromal scores and reduced immune cell infiltration. Immunotherapy response analysis demonstrated that patients with high ADORA2B expression exhibited poorer outcomes following ICB therapy. Drug sensitivity analysis identified several agents, including Ixazomib citrate, Masitinib, and others, as potential therapeutic candidates for high ADORA2B expression patients. In vitro experiments

[†]Pian Li and Ke-ling Pang contributed equally to this work.

*Correspondence:
Man-bo Cai
2018012078@usc.edu.cn
Jun-yan He
junyan_he@126.com

Full list of author information is available at the end of the article

confirmed that ADORA2B knockdown significantly inhibited HNSC cell proliferation, colony formation, and migration, underscoring its critical role in tumor progression.

Conclusion ADORA2B is a key oncogenic driver in HNSC, contributing to tumor proliferation, migration, and an immunosuppressive TME. Its high expression is associated with poor prognosis and reduced immunotherapy efficacy. Targeting ADORA2B may enhance therapeutic outcomes and overcome treatment resistance, highlighting its potential as a diagnostic, prognostic, and therapeutic biomarker.

Keywords ADORA2B, HNSC, Biomarker, Tumor microenvironment, Immunotherapy

Introduction

Head and neck squamous cell carcinoma (HNSC), which encompasses tumors originating in the oral cavity, nasal cavity, pharynx, larynx, neck, and upper esophagus, is recognized as the predominant histological subtype of head and neck cancers, accounting for the vast majority of malignancies arising within this anatomical region [1]. The high incidence of late-stage diagnosis in HNSC patients often leads to local recurrence and distant metastasis, resulting in poor overall survival rates. Despite significant progress in multimodal therapeutic approaches, including surgical resection, radiotherapy, chemotherapy, and immunotherapy, the overall prognosis for HNSC remains unsatisfactory [2]. This is largely due to the complex and multifactorial nature of HNSC pathogenesis, which is driven by genetic mutations, epigenetic alterations, and environmental factors, posing substantial challenges for early detection and effective treatment [3]. Consequently, the identification of novel diagnostic and prognostic biomarkers is crucial for improving patient management.

HNSC is characterized by an immunosuppressive tumor microenvironment (TME), which facilitates immune evasion and aberrant immune signaling, both of which contribute to disease progression [4]. These immunological characteristics not only exacerbate tumor development but also underscore the therapeutic potential of immunotherapy [5]. However, resistance to existing treatment modalities remains a major clinical challenge. Moreover, the initiation, progression, and therapy resistance mechanisms of HNSC are governed by intricate molecular and cellular networks. Although substantial advances have been made in understanding these regulatory pathways, significant knowledge gaps persist regarding the precise molecular mechanisms driving HNSC tumorigenesis and therapeutic resistance [6]. Addressing these knowledge gaps is essential for the identification of novel therapeutic targets, which could ultimately lead to improved treatment strategies and better clinical outcomes.

The adenosine A2B receptor (ADORA2B) is a G protein-coupled receptor encoded on chromosome 17p12, primarily activated by extracellular adenosine. It plays a crucial role in regulating inflammatory responses, hypoxia adaptation, and tumor progression [7–9]. Studies have demonstrated that ADORA2B is highly expressed in various tumor types, where it contributes to tumor proliferation, metastasis, and immune modulation [10–13]. Importantly, ADORA2B activation has been implicated in promoting an immunosuppressive tumor microenvironment through enhanced production of immunosuppressive cytokines, such as IL-6 and IL-10, which facilitate immune evasion [13]. Additionally, evidence indicates that ADORA2B signaling is closely associated with hypoxia-induced tumor progression, further influencing tumor aggressiveness and therapeutic resistance [7–12]. While the role of ADORA2B in other malignancies has been well established, its specific function in HNSC remains largely unexplored, with only limited studies investigating this topic. Recent evidence suggests that ADORA2B activation may contribute to HNSC tumorigenesis by promoting cell proliferation, migration, and vascularization [14]. For instance, pharmacological inhibition of ADORA2B using the inverse agonist PSB-603 significantly suppresses HNSC cell proliferation, migration, and vascular endothelial growth factor A secretion in vitro. These effects are linked to cell cycle arrest and activation of apoptotic pathways. However, while these findings highlight its role in tumor growth and progression, its potential involvement in shaping the immune microenvironment of HNSC remains unexplored. Given the limited number of studies, further investigations are warranted to clarify the functional significance of ADORA2B in HNSC tumorigenesis and its potential role in immune regulation.

In this study, we systematically analyzed the expression profile and clinical significance of ADORA2B in HNSC. Additionally, we developed a nomogram model that integrates ADORA2B expression with clinicopathological parameters to improve prognostic accuracy. To elucidate potential molecular mechanisms, we performed weighted gene co-expression network analysis (WGCNA) and gene ontology (GO) enrichment analysis. Finally, we conducted in vitro cytological experiments to validate the oncogenic role of ADORA2B in HNSC. By combining bioinformatics analysis with experimental validation, this study provides new insights into the role of ADORA2B

in HNSC, which may contribute to the development of more effective therapeutic strategies.

Methods

Data collection

Gene expression datasets were obtained from The Cancer Genome Atlas (TCGA, https://portal.gdc.cancer.gov/) (TCGA-HNSC) and the Gene Expression Omnibus (GEO, https://www.ncbi.nlm.nih.gov/geo/) repositories. The GEO datasets utilized in this study included GSE78060, GSE13601, GSE30784, GSE41613, GSE42743, and GSE145281. Additionally, somatic mutation profiles and clinical data for HNSC patients were extracted from the TCGA database. To ensure the consistency and reliability of the data, all datasets underwent standardized preprocessing, including normalization, log2 transformation, and removal of batch effects.

Differential expression analysis of ADORA2B

To investigate the expression profile of ADORA2B across multiple cancers, a pan-cancer analysis was conducted using the TCGAplot [15] package in R, covering 33 cancer types. For HNSC-specific analysis, ggplot2 (https://CRAN.R-project.org/package=ggplot2) was employed to compare ADORA2B expression levels between tumor and adjacent normal tissues.

Clinical correlation, diagnostic, and prognostic analysis

The relationship between ADORA2B expression and clinicopathological characteristics was analyzed using ggplot2 in R. To assess its diagnostic potential, receiver operating characteristic (ROC) curve analysis was performed, and the area under the curve (AUC) was determined using the pROC [16] package. For prognostic evaluation, univariate Cox regression analysis was conducted via TCGAplot, while Kaplan-Meier survival analysis was performed using the survival (https://CRAN.R-project.org/package=survival) and survminer (https://CRAN.R-project.org/package=survminer) packages in R. The optimal cutoff value for Kaplan-Meier survival analysis was identified using the surv_cutpoint() function in survminer, which determines the most statistically significant threshold for patient stratification based on survival outcomes.

Genomic alteration and mutational burden analysis

The ADORA2B mutation landscape, including mutation frequency, gene amplifications, deletions, and complex alterations, was investigated using the cBioPortal Cancer Type Summary module (https://www.cbioportal.org/). To further examine the relationship between ADORA2B expression and tumor mutation burden (TMB), the maftools [17], ggplot2, and forestPlot [18] packages in R were utilized to compare mutation rates between high and low ADORA2B expression groups.

Development and validation of a nomogram including ADORA2B and clinical characteristics

To enhance prognostic accuracy, a nomogram was constructed by integrating ADORA2B expression with key clinical parameters, including age, clinical T stage, clinical N stage, clinical M stage, overall clinical stage, lymphovascular invasion, and perineural invasion. The rms (https://CRAN.R-project.org/package=rms) package in R was used to generate calibration curves, assessing the agreement between predicted and observed survival probabilities. The predictive performance of the nomogram was further evaluated by computing the concordance index (C-index) and AUC using the riskRegression (https://CRAN.R-project.org/package=riskRegression) and timeROC [19] packages.

WGCNA and functional enrichment analysis

A weighted gene co-expression network was constructed using the WGCNA [20] package in R to identify gene modules correlated with ADORA2B expression in the TCGA dataset. To establish a scale-free topology, a soft threshold power of 12 was applied. Genes exhibiting similar expression patterns were categorized into distinct modules, and the module displaying the strongest correlation with ADORA2B expression was selected for further analysis. Functional annotation and pathway enrichment of the identified module were conducted using the clusterProfiler [21] and org.Hs.eg.db (https://bioconductor.org/packages/org.Hs.eg.db/) packages in R.

Immune infiltration analysis

To characterize immune infiltration and the tumor immune microenvironment, the ESTIMATE [22] package in R was employed to compute immune, stromal, and ESTIMATE scores. The infiltration levels of 28 tumor-infiltrating immune cell types were quantified via single-sample gene set enrichment analysis (ssGSEA) using the GSVA [23] package. Wilcoxon test and Pearson correlation analysis was performed to assess the relationship between ADORA2B expression and immune cell infiltration.

Drug sensitivity analysis

The correlation between ADORA2B expression and drug sensitivity was examined using the NCI-60 cell line panel, which includes 60 tumor cell lines and sensitivity data for 792 chemotherapeutic and targeted agents. Cell lines with over 60% missing data were excluded from the analysis. Wilcoxon test and Pearson correlation analysis was conducted to explore the association between ADORA2B expression and drug sensitivity.

Cell culture

The HNSC cell lines SAS and SCC-9 were purchased from the Cell Bank of Chinese Academy of Sciences (Shanghai, China). SAS cells were cultured in DMEM (Gibco, USA), and SCC-9 cells were cultured in DMEM/F12 (Gibco, USA). Both media were supplemented with 10% fetal bovine serum (FBS, Gibco, USA) and 1% penicillin-streptomycin solution (P1400, Solarbio, China). The HNSCC cells were incubated at 37 °C in a humidified atmosphere with 5% CO_2.

RNA extraction and quantitative RT-PCR analysis

Total RNA was extracted from HNSCC cells using the SevenFast® Total RNA Extraction Kit for Cells (SM130, SevenBio, China) following the manufacturer's instructions. The RNA concentration was measured using the NanoDrop One spectrophotometer (Thermo Fisher, USA). cDNA synthesis was performed using the TransScript® Uni All-in-One First-Strand cDNA Synthesis SuperMix for qPCR (One-Step gDNA Removal) (AU341, Transgen, China) following the manufacturer's guidelines. Finally, gene expression was quantified using the SYBR Green Mix (A25742, Thermo Fisher, USA) on the Quant Studio™ 6 Real-Time PCR System (Thermo Fisher, USA), with the following parameters: pre-denaturation at 50 °C for 2 min, followed by 95 °C for 10 min (1 cycle); 95 °C for 15 s, 60 °C for 1 min (40 cycles). GAPDH was used as the internal control. Relative gene expression was calculated using the 2-ΔΔCt method. The qPCR primer sequences are as follows:

ADORA2B:

5′- TGCACTGACTTCTACGGCTG – 3′ (forward).

5′- GGTCCCCGTGACCAAACTT – 3′(reverse).

GAPDH:

5′- TTGCCATCAATGACCCCTTCA – 3′ (forward).

5′- CGCCCCACTTGATTTTGGA-3′(reverse).

ADORA2B knockdown

To knock down ADORA2B expression, a control siRNA and three specific small interfering RNAs (siRNAs) targeting the ADORA2B mRNA sequence were identified and synthesized by GenePharma (Suzhou, China). The sequences of the siRNAs used are listed in the table below. When the cells reached 70% confluence, the siRNAs (si-control and si-ADORA2B) were transfected into SAS and SCC-9 cells using Lipofectamine 3000 (L3000015, Thermo Fisher, USA) according to the manufacturer's instructions. The sequences of the siRNAs used are listed as follows:

si-NC:

(sense: 5′- UUCUCCGAACGUGUCACGUTT – 3′; antisense: 5′- ACGUGACACGUUCGGAGAATT – 3′)

ADORA2B-siRNA-1:

(sense: 5′- GCUUCGUGCUGGUGCUCACTT – 3′; antisense: 5′- GUGAGCACCAGCACGAAGCTT – 3′)

ADORA2B-siRNA-2:

(sense: 5′ - CAGUUGUCAAUCCCAUUGUTT – 3′; antisense: 5′- ACAAUGGGAUUGACAACUGTT – 3′)

ADORA2B-siRNA-3:

(sense: 5′ - GUGAAAGAUAGCUACACCUTT – 3′; antisense: 5′- AGGUGUAGCUAUCUUUCACTT – 3′)

Cell proliferation assay

Cell proliferation was assessed using the CCK-8 assay. SAS and SCC-9 cells transfected with si-control or si-ADORA2B were resuspended in complete culture medium and seeded into 96-well plates at a density of 2000 cells per well. The cells were cultured for the specified time periods. After discarding the original medium, 100 μL of CCK-8 working solution was added to each well, consisting of 10 μL CCK-8 solution (BS350A, Biosharp, China) and 90 μL culture medium. Following the manufacturer's instructions, cells were incubated in a 37 °C incubator for 1 h. The optical density (OD) was measured at 450 nm using a spectrophotometer.

Colony formation assay

SAS and SCC-9 cells transfected with si-control or si-ADORA2B were resuspended in complete culture medium and seeded into 12-well plates at a density of 2000 cells per well. Cells were cultured for 7 days in a 37 °C incubator with 5% CO_2 and saturated humidity. Cells were fixed with 4% paraformaldehyde (P1110, Solarbio, China) at room temperature for 30 min, and then stained with crystal violet (G1062, Solarbio, China) at room temperature for 30 min. Colony images were captured using a camera, and the number of colonies was counted using ImageJ software.

Migration assays

Ibidi chambers (80209, Ibidi, Germany) were affixed to the center of 12-well plates. SAS and SCC-9 cells transfected with si-control or si-ADORA2B were resuspended in complete culture medium and seeded into the small chambers of the Ibidi chamber at a density of 4 × 10^4 cells per chamber. Once the cells adhered, the Ibidi chamber was removed. Cell migration was observed at 0 h, 6 h, and 9 h under an inverted microscope, and images were taken. Wound healing was measured using ImageJ software, and the healing rate was calculated as follows: Wound healing rate = (0 h area - n h area) / (0 h area) × 100%.

Statistical analysis

All statistical analyses were conducted using R software (version 4.2.2), with $p < 0.05$ considered statistically significant. Experimental data were analyzed

using GraphPad Prism (version 9.5). To ensure analytical robustness, each experiment was performed with a minimum of three independent replicates, and statistical differences were evaluated using the t-test. Statistical significance was denoted as $^{*}P < 0.05$, $^{**}P < 0.01$, $^{***}P < 0.001$, and $^{****}P < 0.0001$.

Results

Elevated ADORA2B expression in HNSC

To investigate ADORA2B expression across different malignancies, we conducted differential expression analysis comparing tumor and normal tissues. As shown in Fig. 1a, ADORA2B was found to be significantly upregulated in multiple cancer types, including cervical squamous cell carcinoma and endocervical adenocarcinoma (CESC), cholangiocarcinoma (CHOL), esophageal carcinoma (ESCA), HNSC, kidney renal clear cell carcinoma (KIRC), liver hepatocellular carcinoma (LIHC), lung adenocarcinoma (LUAD), lung squamous cell carcinoma (LUSC), prostate adenocarcinoma (PAAD), and stomach adenocarcinoma (STAD). Further paired analysis of tumor and adjacent normal tissues confirmed significant overexpression of ADORA2B in ESCA, HNSC, KIRC, LUAD, LUSC, and STAD (Fig. 1b), with HNSC exhibiting one of the highest ADORA2B expression levels among these cancer types (Fig. 1c). Notably, ADORA2B expression in HNSC was markedly elevated ($p < 0.0001$, Fig. 1d-e). ROC curve analysis further demonstrated that ADORA2B expression could effectively differentiate HNSC from normal tissues, with an AUC of 0.732 (95% CI: 0.652–0.801), suggesting its potential as a diagnostic biomarker for HNSC (Fig. 1f). These findings were validated using independent GEO datasets (GSE78060, GSE13601, and GSE30784), which consistently corroborated the results obtained from the TCGA dataset (Fig. 1g-i).

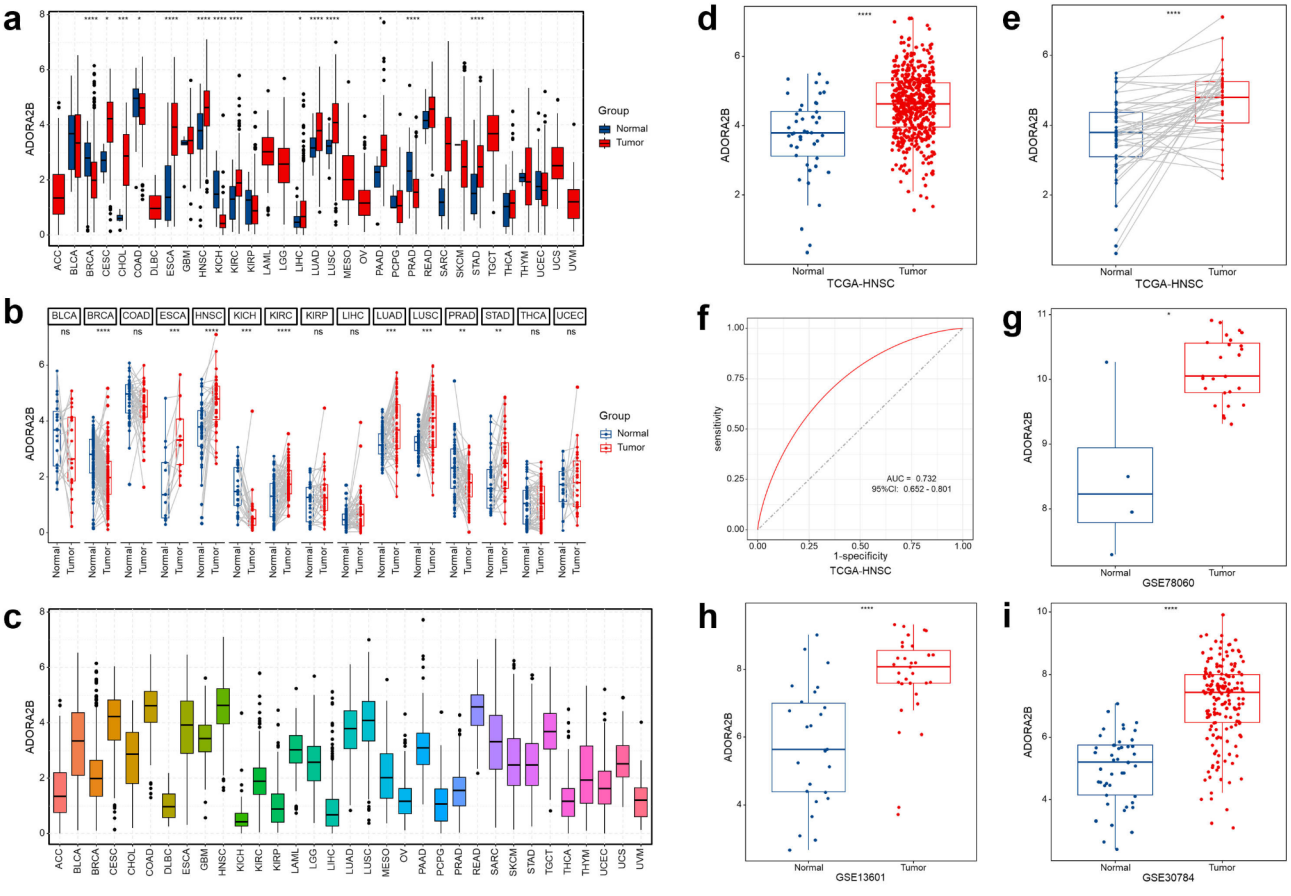

Fig. 1 Elevated ADORA2B expression in HNSC and multiple cancer types. Pan-cancer analysis of ADORA2B expression in normal and tumor tissues from TCGA datasets (**a**). Paired analysis of ADORA2B expression in tumor and adjacent normal tissues from TCGA datasets (**b**). Comparative analysis of ADORA2B expression across multiple cancer types (**c**). Boxplot and paired plot of ADORA2B expression in HNSC tumor and normal tissues from TCGA datasets (**d**, **e**). ROC curve analysis of ADORA2B expression in HNSC (**f**). Independent validation of ADORA2B expression in HNSC using GSE78060 (**g**), GSE13601 (**h**), and GSE30784 (**i**) datasets. Abbreviations: TCGA, The Cancer Genome Atlas; HNSC, head and neck squamous cell carcinoma; ROC, receiver operating characteristic. Statistical significance: $^{*}p < 0.05$, $^{**}p < 0.01$, $^{***}p < 0.001$, $^{****}p < 0.0001$, ns: not significant

Correlation between ADORA2B expression and clinical features in HNSC

To explore the clinical relevance of ADORA2B expression, we analyzed its association with clinicopathological parameters using the TCGA database. The results revealed that higher ADORA2B expression was significantly correlated with more advanced clinical and pathological stages, including clinical T stage, overall clinical stage, pathologic T stage, and pathologic stage (Fig. 2a-l). Specifically, patients with more advanced clinical or pathological T and overall stages exhibited markedly increased ADORA2B expression levels. These findings suggest that ADORA2B is associated with adverse clinical characteristics in HNSC and may serve as a prognostic biomarker linked to poor outcomes.

Prognostic significance of ADORA2B in HNSC

To further assess the prognostic value of ADORA2B, survival analysis was conducted. As illustrated in Fig. 3a, high ADORA2B expression was associated with poor prognosis in multiple cancers, including HNSC, KIRC, lower-grade glioma (LGG), mesothelioma (MESO), and PAAD. Kaplan-Meier survival analysis demonstrated that HNSC patients with elevated ADORA2B expression had significantly shorter overall survival (OS) (Fig. 3b) and progression-free survival (PFS) (Fig. 3c). Furthermore, independent validation using GEO datasets (GSE41613 and GSE42743) confirmed that higher ADORA2B expression was linked to worse OS in HNSC patients (Fig. 3d-e). These consistent findings across datasets highlight the robust prognostic significance of ADORA2B in HNSC.

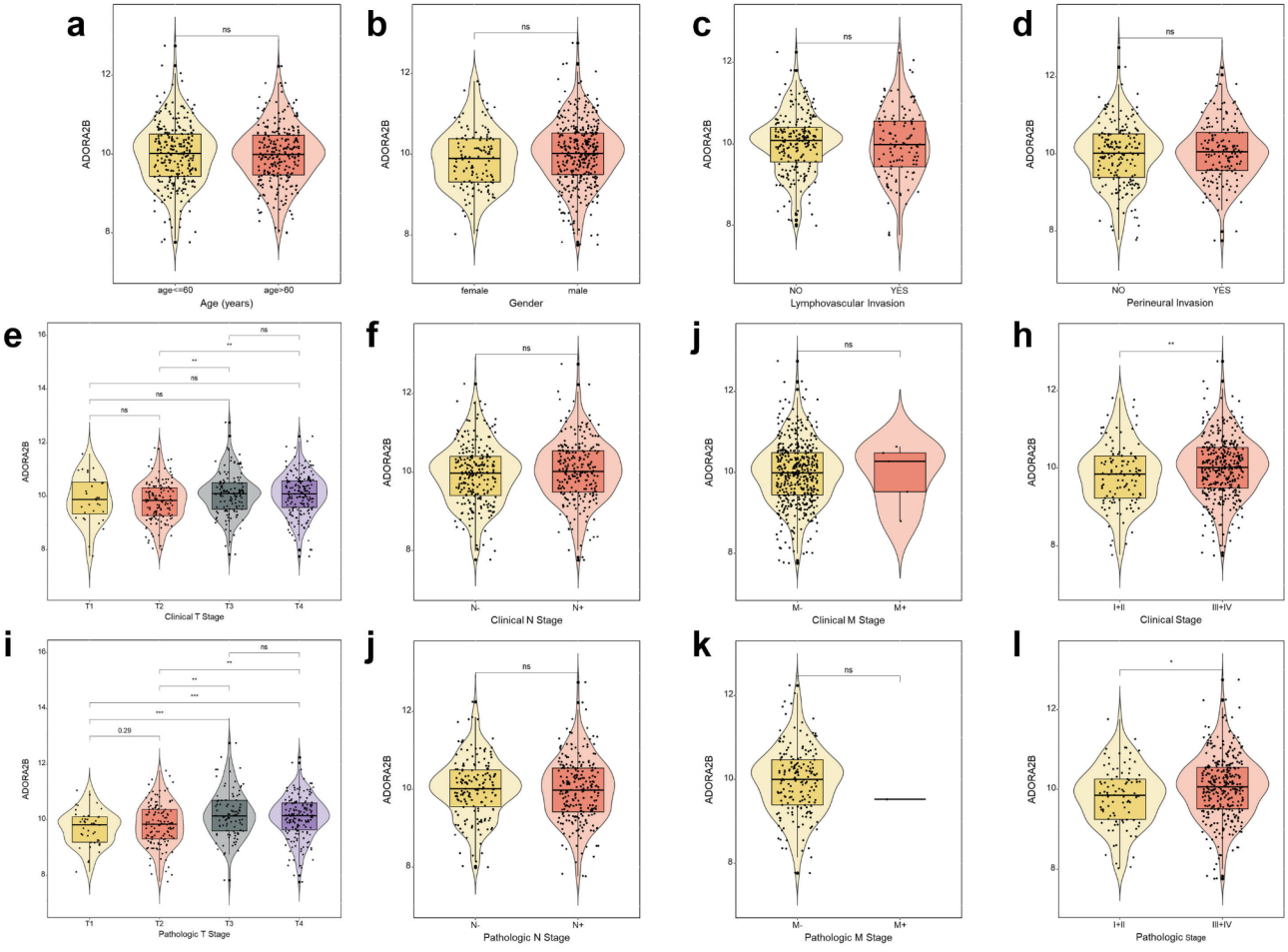

Fig. 2 Correlation between ADORA2B expression and clinical features in HNSC. Violin plots showing the relationship between ADORA2B expression and age (**a**), gender (**b**), lymphovascular invasion (**c**), and perineural invasion (**d**) in HNSC patients from TCGA datasets. (**e**-**h**) Association of ADORA2B expression with clinical T stage (**e**), clinical N stage (**f**), clinical M stage (**g**), and overall clinical stage (**h**). (**i**-**l**) Correlation between ADORA2B expression and pathological T stage (**i**), pathological N stage (**j**), pathological M stage (**k**), and overall pathological stage (**l**). Abbreviations: TCGA, The Cancer Genome Atlas; HNSC, head and neck squamous cell carcinoma. Statistical significance: *$p < 0.05$, **$p < 0.01$, ***$p < 0.001$, ****$p < 0.0001$, ns: not significant

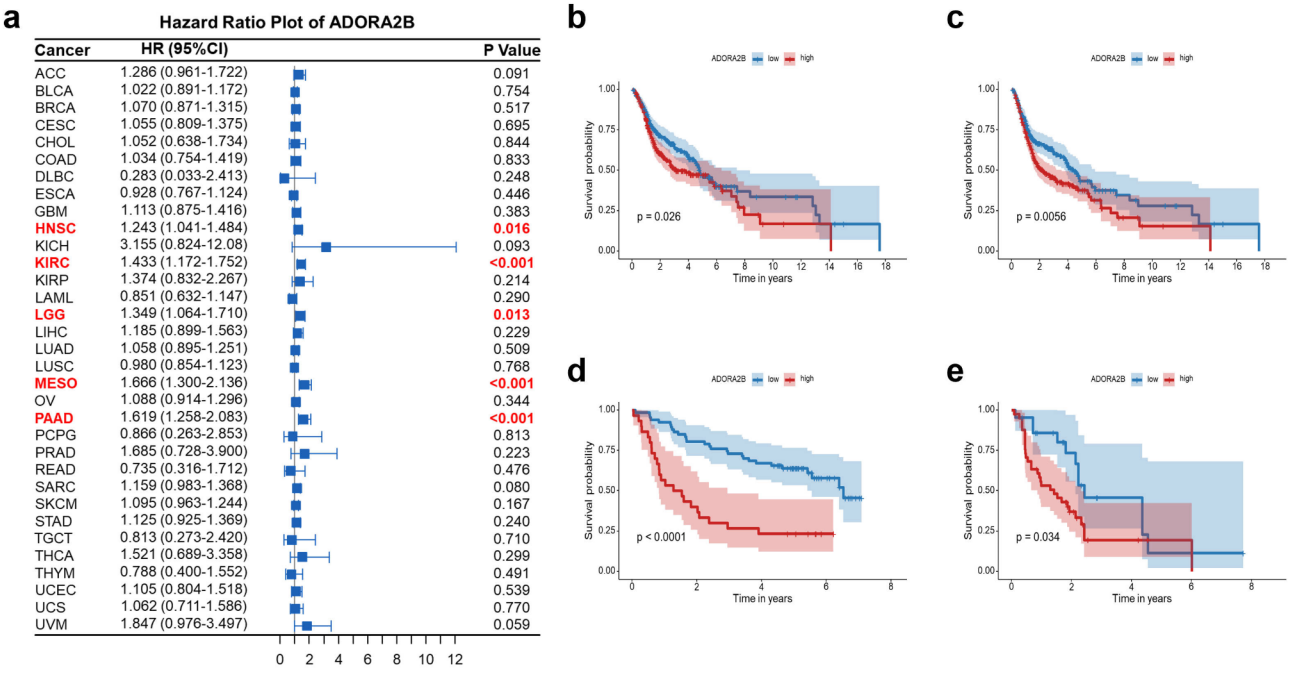

Fig. 3 Prognostic significance of ADORA2B in HNSC. Pan-cancer univariate Cox regression analysis of ADORA2B expression from TCGA datasets (**a**). Kaplan-Meier survival analysis of OS (**b**) and PFS (**c**) in HNSC patients from TCGA datasets. Kaplan-Meier survival analysis of OS in HNSC patients from the GSE41613 (**d**) and GSE42743 (**e**) dataset. Abbreviations: TCGA, The Cancer Genome Atlas; HNSC, head and neck squamous cell carcinoma; OS, overall survival; PFS, progression-free survival

Genomic alterations analysis

The genetic alteration landscape of ADORA2B was explored using cBioPortal (Fig. 4a). Among various cancers, sarcoma exhibited the highest alteration frequency, predominantly characterized by amplification mutations. However, in HNSC, ADORA2B mutations were rare, with less than 1% of patients displaying amplification mutations. To further examine the functional impact of these mutations, we analyzed their relationship with ADORA2B expression levels (Figs. 4b-c). The results indicated comparable mutation rates between high- and low-ADORA2B expression groups, with a slight increase in mutation rates observed in the high-expression group. Differential mutation profiles between high and low ADORA2B expression groups are depicted in Fig. 4d, with genes such as HRAS, AFF3, PALM2AKAP2, PKHD1L1, COL3A1, HDAC9, SLC8A3, AMPH, AJUBA, TP53, and SORCS1 exhibiting a higher mutation frequency in the high-expression group ($p < 0.05$). Conversely, mutations in DDR2, PCNX1, NTRK3, KDM6A, AKAP13, KIF26B, OR2M5, COL19A1, NLRP12, WDFY3, and CELSR2 were more prevalent in low ADORA2B expression patients ($p < 0.05$). Additionally, Kaplan-Meier survival analysis revealed that patients with both high ADORA2B expression and high TMB had the poorest survival outcomes (Fig. 4e).

ADORA2B based nomogram and relevant evaluation

To improve prognostic prediction accuracy, we constructed a nomogram incorporating ADORA2B expression along with clinicopathological factors, including age, clinical T stage, clinical N stage, clinical M stage, overall clinical stage, lymphovascular invasion, and perineural invasion, within the TCGA cohort (Fig. 5a). Calibration curves for 1-, 3-, and 5-year OS demonstrated that the nomogram predictions closely aligned with actual survival outcomes (Fig. 5b). The C-index of the nomogram was notably higher compared to using ADORA2B expression alone (Fig. 5c). Kaplan-Meier survival analysis further indicated that patients with high nomogram scores had significantly worse OS (Fig. 5d). The ROC AUC values for predicting 1-, 3-, and 5-year OS were 0.698, 0.767, and 0.722, respectively, underscoring the strong predictive performance of the ADORA2B-based nomogram (Fig. 5e).

WGCNA analysis and functional enrichment analysis

To explore potential regulatory mechanisms of ADORA2B in HNSC, we constructed a WGCNA network using the TCGA dataset. By applying a soft threshold power of 12, we identified 10 distinct gene modules based on the topological overlap matrix (TOM) (Fig. 6a). These modules were categorized as turquoise (2831 genes), black (725), red (1213), blue (2317), green (1271), brown (1263), pink (594), magenta (201), yellow (1462),

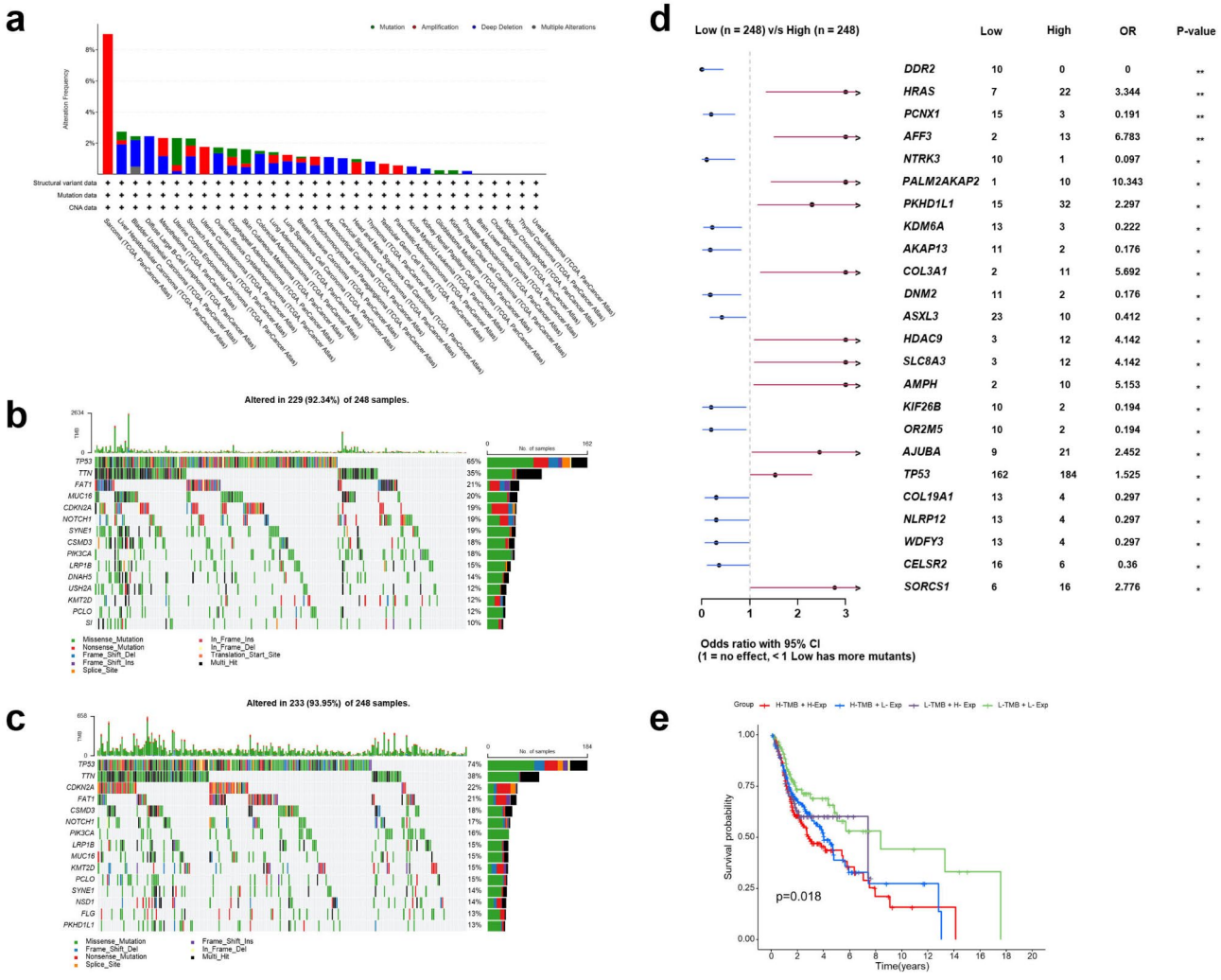

Fig. 4 Genomic alterations of ADORA2B in HNSC. Genetic alteration landscape of ADORA2B across multiple cancer types from cBioPortal (**a**). Oncoplots displaying the mutational profiles of high- and low-ADORA2B expression groups in HNSC (**b**, **c**). Differential mutation analysis between high- and low-ADORA2B expression groups, highlighting significantly altered genes (**d**). Kaplan-Meier survival analysis of HNSC patients stratified by ADORA2B expression and TMB (**e**). Abbreviations: HNSC, head and neck squamous cell carcinoma; TMB, tumor mutational burden; OR, odds ratio; CI, confidence interval. Statistical significance: *$p < 0.05$, **$p < 0.01$, ***$p < 0.001$, ****$p < 0.0001$, ns: not significant

and grey (5060) (Fig. 6b). Among them, the yellow module exhibited the strongest negative correlation with ADORA2B expression (correlation coefficient = -0.45, $p = 8.5e\text{-}74$, Fig. 6b-c). GO analysis revealed that genes in the yellow module were primarily enriched in biological processes (BP) related to leukocyte-mediated immunity, regulation of immune effector processes, and lymphocyte differentiation (Fig. 6d, top). Regarding cellular components (CC), these genes were predominantly associated with the external side of the plasma membrane, secretory granule membrane, and tertiary granule (Fig. 6d, middle). Molecular function (MF) analysis indicated that these genes were involved in immune receptor activity, cytokine receptor binding, and carbohydrate binding (Fig. 6d, bottom). Furthermore, Kyoto encyclopedia of genes and genomes (KEGG) pathway analysis identified significant enrichment in cytokine-cytokine receptor interaction, intestinal immune network for IgA production, chemokine signaling pathway, primary immune deficiency, and hematopoietic cell lineage (Fig. 6e). Hallmark pathway enrichment analysis further demonstrated that genes in the yellow module were predominantly involved in immune-related processes, including allograft rejection, inflammatory response, interferon-gamma response, complement activation, IL2-STAT5 signaling, and IL6-JAK-STAT3 signaling (Fig. 6f). These findings highlight the potential role of ADORA2B in modulating immune-related pathways within the HNSC microenvironment.

To explore the potential mechanisms through which ADORA2B promotes tumor growth and migration, we performed GSEA by stratifying HNSC patients into high and low ADORA2B expression groups based on

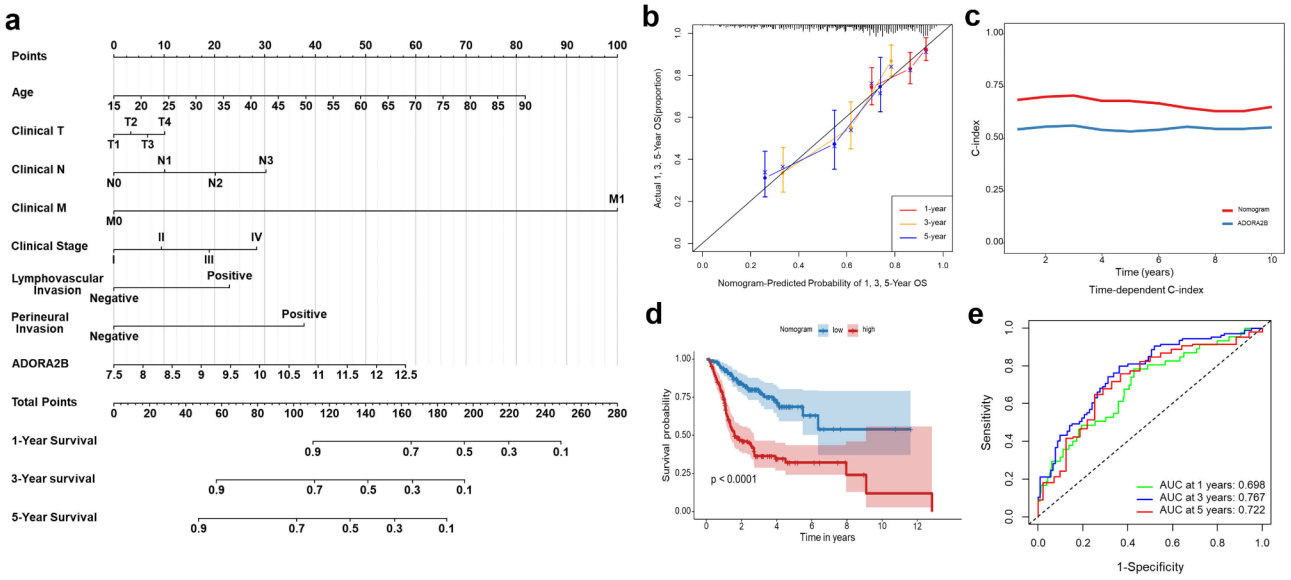

Fig. 5 ADORA2B-based nomogram and prognostic evaluation in HNSC. Nomogram integrating ADORA2B expression and clinicopathological factors for predicting 1-, 3-, and 5-year OS in HNSC patients (**a**). Calibration curves showing the agreement between nomogram-predicted and actual survival probabilities at 1, 3, and 5 years (**b**). Time-dependent C-index comparison between the nomogram and ADORA2B expression alone (**c**). Kaplan-Meier survival analysis of HNSC patients stratified by nomogram scores (**d**). ROC curves for the nomogram predicting 1-, 3-, and 5-year OS (**e**). Abbreviations: HNSC, head and neck squamous cell carcinoma; OS, overall survival; Concordance index, C-index; ROC, receiver operating characteristic

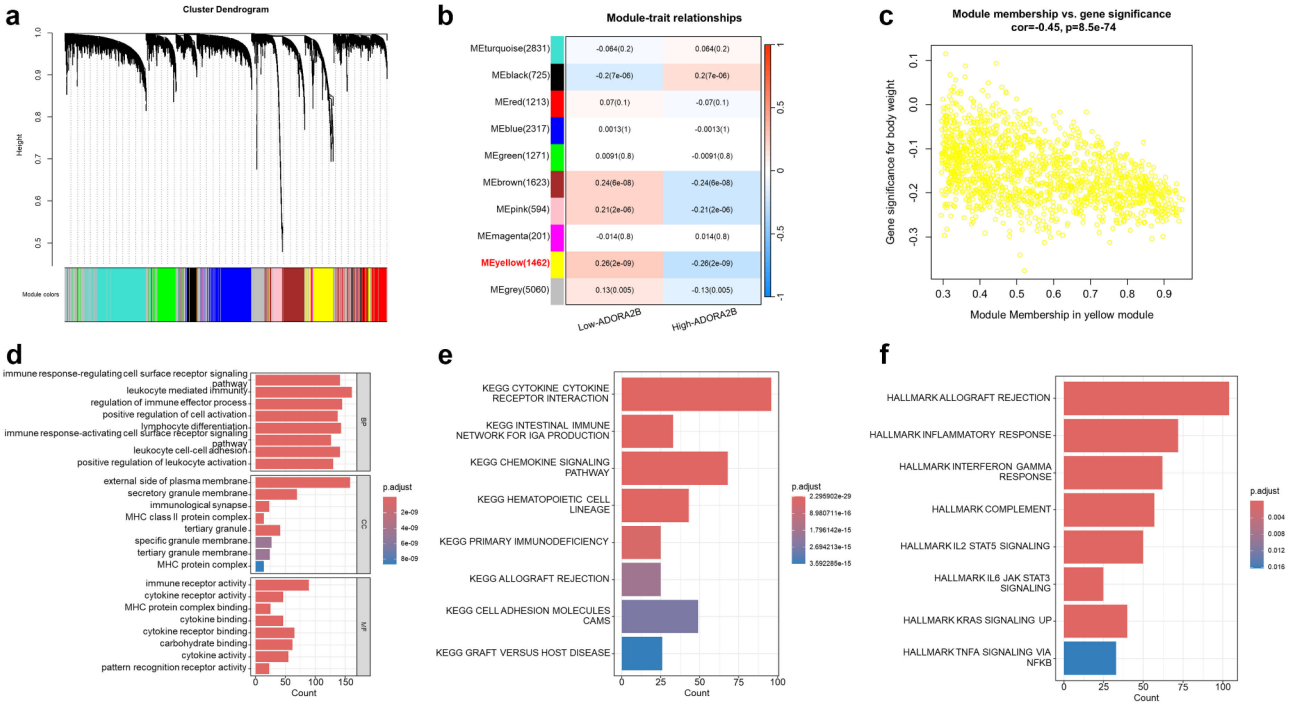

Fig. 6 WGCNA analysis and functional enrichment of ADORA2B-associated gene modules in HNSC. Cluster dendrogram of co-expressed genes in HNSC, with different colors representing distinct gene modules identified by WGCNA (**a**). Module-trait relationships showing the correlation between gene modules and ADORA2B expression (**b**). Scatter plot of gene significance versus module membership in the yellow module (**c**). Gene Ontology (GO) enrichment analysis of genes in the yellow module (**d**). KEGG pathway enrichment analysis of genes in the yellow module (**e**). Hallmark pathway enrichment analysis showing immune-related pathways associated with the yellow module (**f**) Abbreviations: WGCNA, weighted gene co-expression network analysis; HNSC, head and neck squamous cell carcinoma; GO, Gene Ontology; KEGG, Kyoto Encyclopedia of Genes and Genomes

the median expression level. The results revealed that several hallmark oncogenic pathways were significantly activated in the high-ADORA2B group, including MYC targets, E2F targets, G2M checkpoint, mTORC1 signaling, and DNA repair pathways (Figure S1). These findings suggest that ADORA2B may facilitate tumor proliferation by enhancing cell cycle progression (E2F and G2M checkpoint), promoting metabolic adaptation (mTORC1 signaling), and increasing genomic stability (DNA repair pathways). Additionally, pathways related to hypoxia, TNFα signaling via NF-κB, and glycolysis were also enriched, indicating that ADORA2B may contribute to tumor aggressiveness and immune modulation.

ADORA2B is involved in immune cell infiltration in HNSC

Given the WGCNA and functional enrichment findings, which indicated a potential role of ADORA2B in immune regulation, we performed a comprehensive immune infiltration analysis to assess differences between high- and low-ADORA2B expression groups in HNSC. First, we compared immune scores, stromal scores, and ESTIMATE scores to evaluate the overall immune status in patients with high versus low ADORA2B expression. As expected, patients with high ADORA2B expression exhibited significantly lower immune, stromal, and ESTIMATE scores, indicating a more immunosuppressive tumor microenvironment (Fig. 7a). This observation highlights the potential immunosuppressive role of ADORA2B in HNSC. To further elucidate the relationship between ADORA2B and tumor-infiltrating immune

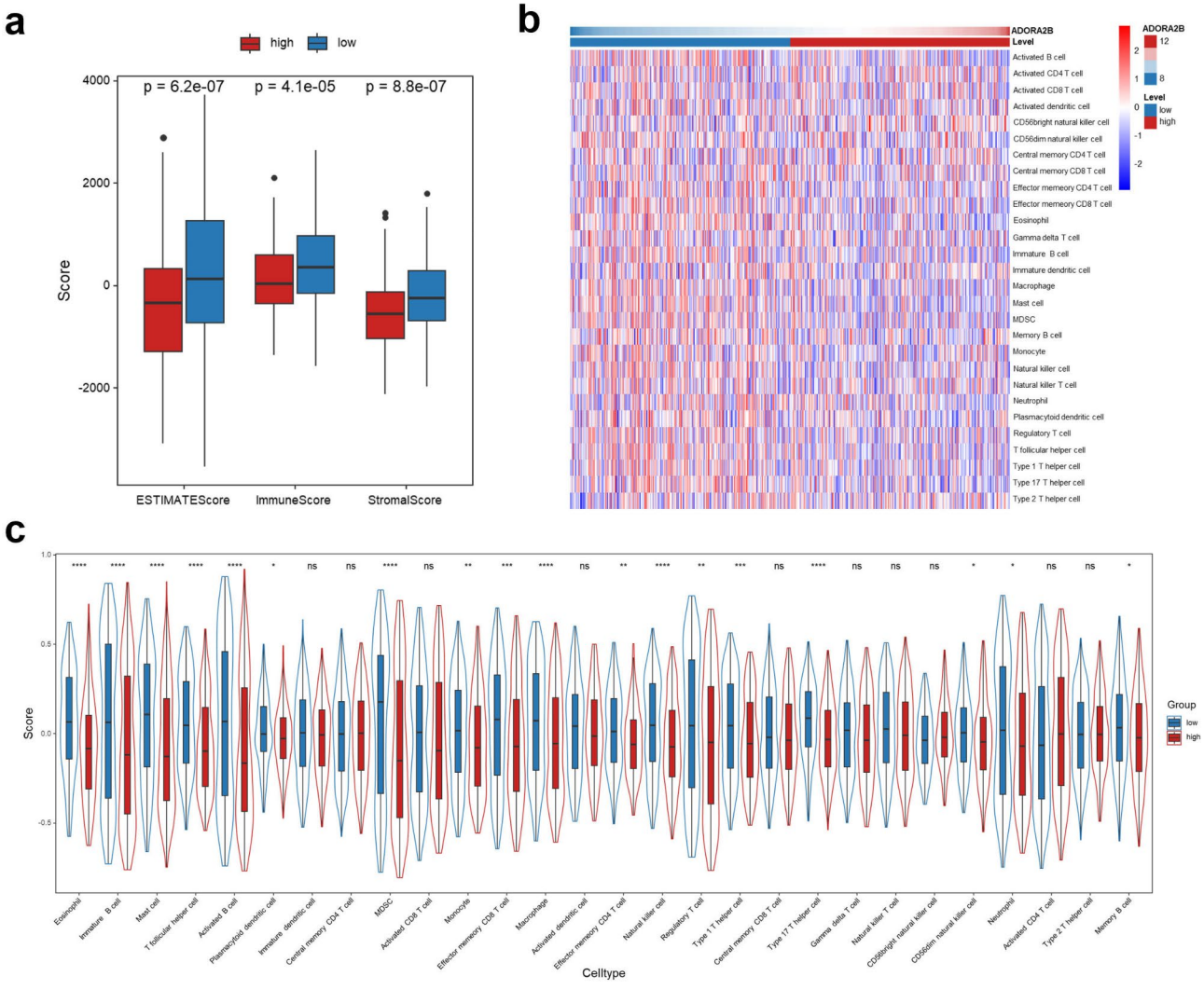

Fig. 7 ADORA2B is involved in immune cell infiltration in HNSC. Boxplots comparing ESTIMATE scores, immune scores, and stromal scores between high- and low-ADORA2B expression groups in HNSC (**a**). Heatmap of the infiltration of various immune cell types in low- and high-ADORA2B expression groups (**b**). Violin plots comparing the infiltration levels of various immune cell types between high- and low-ADORA2B expression groups (**c**). Abbreviations: HNSC, head and neck squamous cell carcinoma. Statistical significance: *$p < 0.05$, **$p < 0.01$, ***$p < 0.001$, ****$p < 0.0001$, ns: not significant

cells, we performed ssGSEA. The results, illustrated in Fig. 7b, revealed that high ADORA2B expression was associated with significantly reduced infiltration of most immune cell types compared to the low-expression group. Specifically, 18 immune cell types exhibited significantly lower infiltration levels in the high-ADORA2B expression group (Fig. 7c). Further Pearson correlation analysis demonstrated that ADORA2B expression was negatively correlated with the majority of immune cell populations (Fig. 8a). A detailed correlation analysis of specific immune cells negatively associated with ADORA2B expression (cor < -0.1, $p < 0.01$) is presented in Figs. 8b-p. These findings suggest that ADORA2B may contribute to immune evasion in HNSC by reducing immune cell infiltration.

Correlation analysis of ADORA2B expression with immunotherapy response

To further investigate the potential role of ADORA2B in immunotherapy response, we analyzed its relationship with immune checkpoint molecules and immune checkpoint blockade (ICB) treatment outcomes. Our analysis revealed that immune checkpoint expression levels were significantly higher in the low-ADORA2B expression group (Fig. 9a), suggesting that patients with lower ADORA2B expression may exhibit greater responsiveness to ICB therapy. To validate these findings, we stratified participants in the IMvigor210 immunotherapy cohort (GSE145281) into high- and low-ADORA2B expression groups. As hypothesized, patients in the low-ADORA2B expression group demonstrated significantly improved survival outcomes following ICB treatment compared to those with high ADORA2B expression (Fig. 9b). Moreover, patients who achieved a complete or partial response to ICB therapy exhibited notably lower ADORA2B expression levels compared to those with stable or progressive disease (Fig. 9c). These results suggest that ADORA2B expression may serve as a predictive biomarker for immunotherapy response, with lower expression levels potentially indicating better treatment outcomes.

Correlation between ADORA2B expression and drug sensitivity

To identify potential therapeutic agents for patients with high ADORA2B expression, we assessed the correlation between ADORA2B expression levels and drug sensitivity. Our analysis revealed a negative correlation between ADORA2B expression and sensitivity to several anticancer drugs, including Ixazomib citrate, Homoharringtonine, Masitinib, Pevonedistat, Amuvatinib, Arsenic trioxide, Parthenolide, and Imetelstat (Figs. 10a-b). These findings suggest that targeting these drugs could offer a

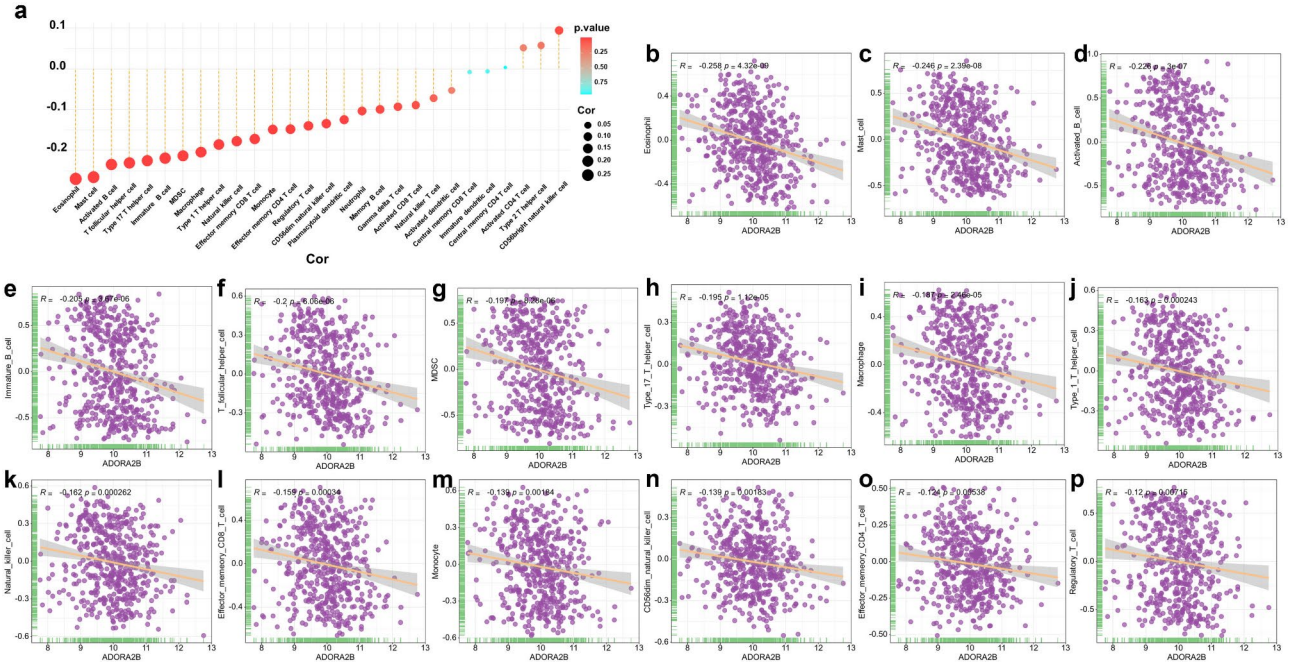

Fig. 8 Correlation between ADORA2B expression and immune cell infiltration in HNSC. Correlation analysis between ADORA2B expression and various immune cell types in HNSC (**a**). (**b**–**p**) Scatter plots showing the negative correlation between ADORA2B expression and specific immune cell populations, including eosinophils (**b**), mast cells (**c**), activated B cells (**d**), immature B cells (**e**), T follicular helper cells (**f**), MDSCs (**g**), type 1 T helper cells (**h**), macrophages (**i**), type 17 T helper cells (**j**), natural killer cells (**k**), effector memory CD8 T cells (**l**), monocytes (**m**), CD56dim natural killer cells (**n**), effector memory CD4 T cells (**o**), and regulatory T cells (**p**). Abbreviations: HNSC, head and neck squamous cell carcinoma; MDSCs, myeloid-derived suppressor cells

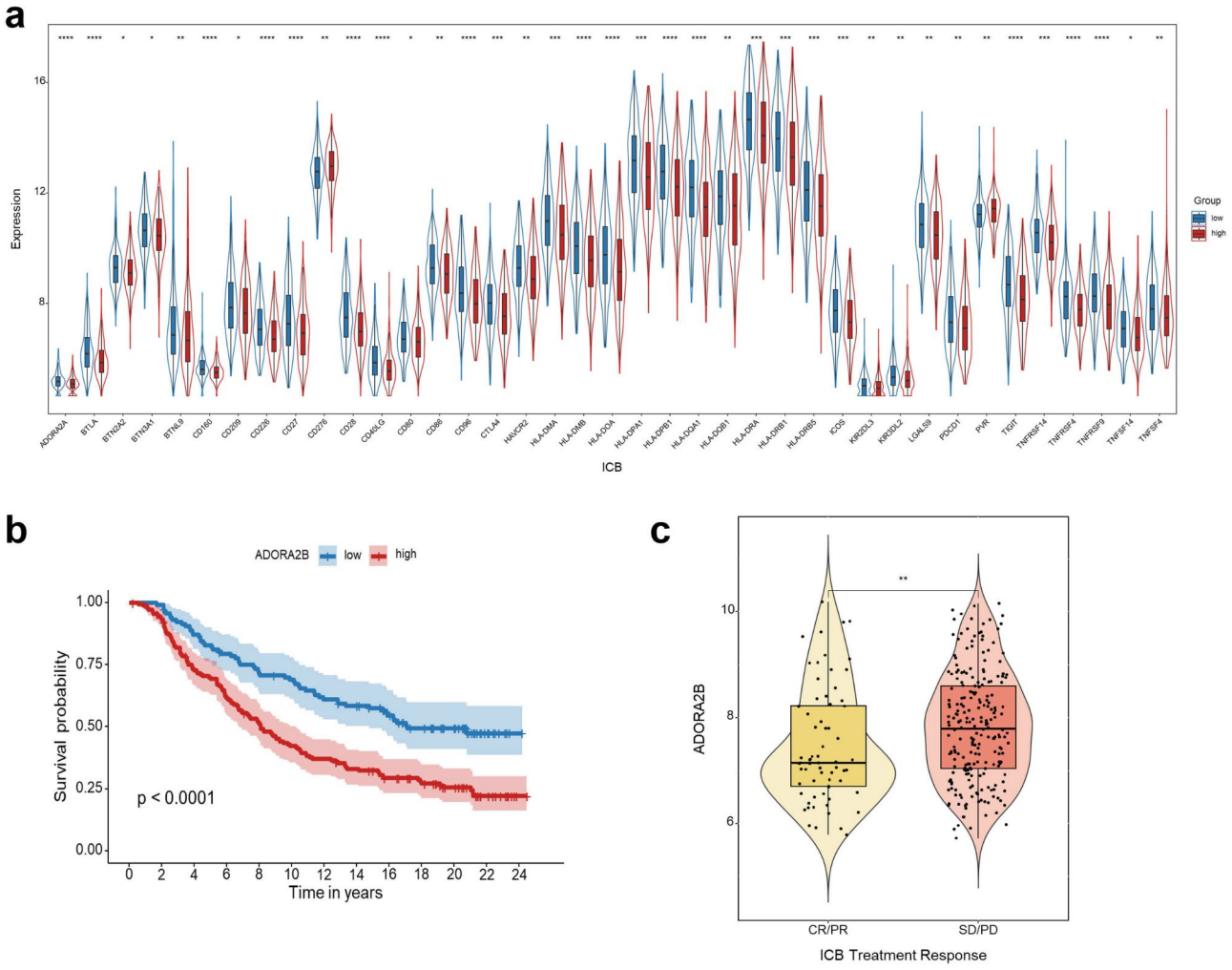

Fig. 9 Correlation between ADORA2B expression and immunotherapy response. Violin plots comparing the expression levels of immune checkpoint molecules between high- and low-ADORA2B expression groups in HNSC patients (**a**). Kaplan-Meier survival analysis of patients from the IMvigor210 cohort (GSE145281) stratified by ADORA2B expression, showing improved survival outcomes in the low-ADORA2B expression group following ICB therapy (**b**). Violin plot comparing ADORA2B expression levels between patients with CR/PR and those with SD/PD after ICB treatment (**c**). Abbreviations: HNSC, head and neck squamous cell carcinoma; ICB, immune checkpoint blockade; CR, complete response; PR, partial response; SD, stable disease; PD, progressive disease. Statistical significance: *$p < 0.05$, **$p < 0.01$, ***$p < 0.001$, ****$p < 0.0001$, ns: not significant

promising strategy to improve therapeutic outcomes in patients with elevated ADORA2B expression.

Knockdown ADORA2B inhibits the proliferation and migration of HNSC cells

To validate the functional role of ADORA2B in HNSC, we performed siRNA-mediated knockdown experiments in SAS and SCC-9 cells. Successful knockdown of ADORA2B was confirmed via qRT-PCR analysis (Fig. 11a). CCK-8 assays demonstrated that silencing ADORA2B significantly inhibited HNSC cell proliferation (Fig. 11b-c). In addition, colony formation assays showed that ADORA2B knockdown markedly reduced the colony-forming ability of HNSC cells (Fig. 11d-e). Furthermore, wound healing assays revealed that ADORA2B knockdown significantly impaired HNSC cell migration, indicating its role in tumor cell motility (Fig. 11f-g). These findings collectively suggest that ADORA2B plays a critical role in promoting HNSC cell proliferation and migration, and that its inhibition may serve as a potential therapeutic strategy.

Discussion

HNSC is among the most prevalent and aggressive malignancies worldwide [1]. Despite advances in multimodal treatment approaches, including surgery, radiotherapy, and chemotherapy, the prognosis for HNSC patients remains unsatisfactory [2]. Immunotherapy, particularly ICB treatment, has revolutionized the treatment landscape for recurrent or metastatic HNSC, demonstrating superior clinical efficacy compared to conventional chemotherapy [5, 24]. Notably, recent clinical trials have

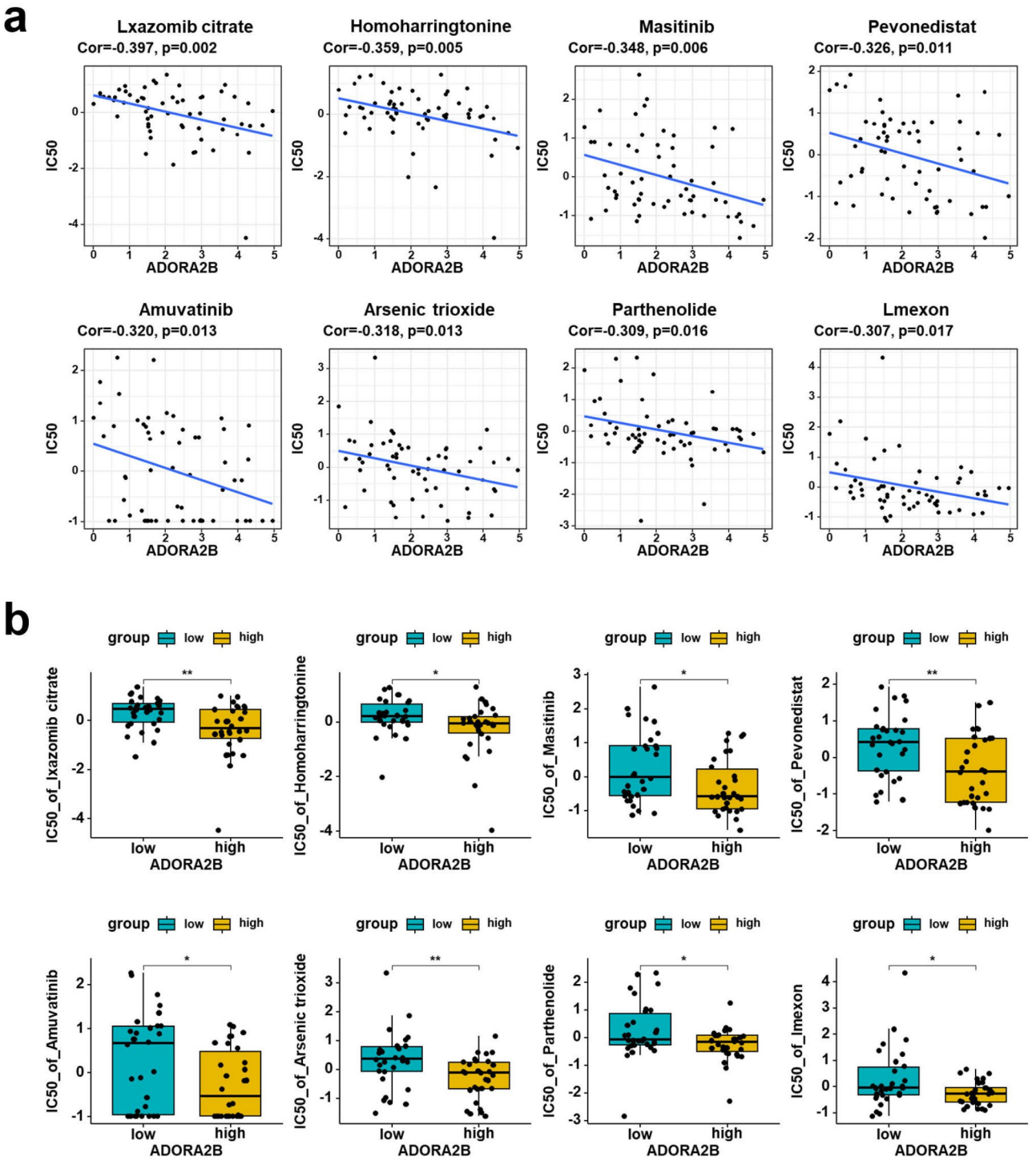

Fig. 10 Correlation between ADORA2B expression and drug sensitivity. Scatter plots showing the negative correlation between ADORA2B expression and IC50 values of various anticancer drugs, including Ixazomib citrate, Homoharringtonine, Masitinib, Pevonedistat, Amuvatinib, Arsenic trioxide, Parthenolide, and Imetelstat (**a**). Boxplots comparing IC50 values of these drugs between high- and low-ADORA2B expression groups (**b**). Statistical significance: *$p < 0.05$, **$p < 0.01$, ***$p < 0.001$, ****$p < 0.0001$, ns: not significant

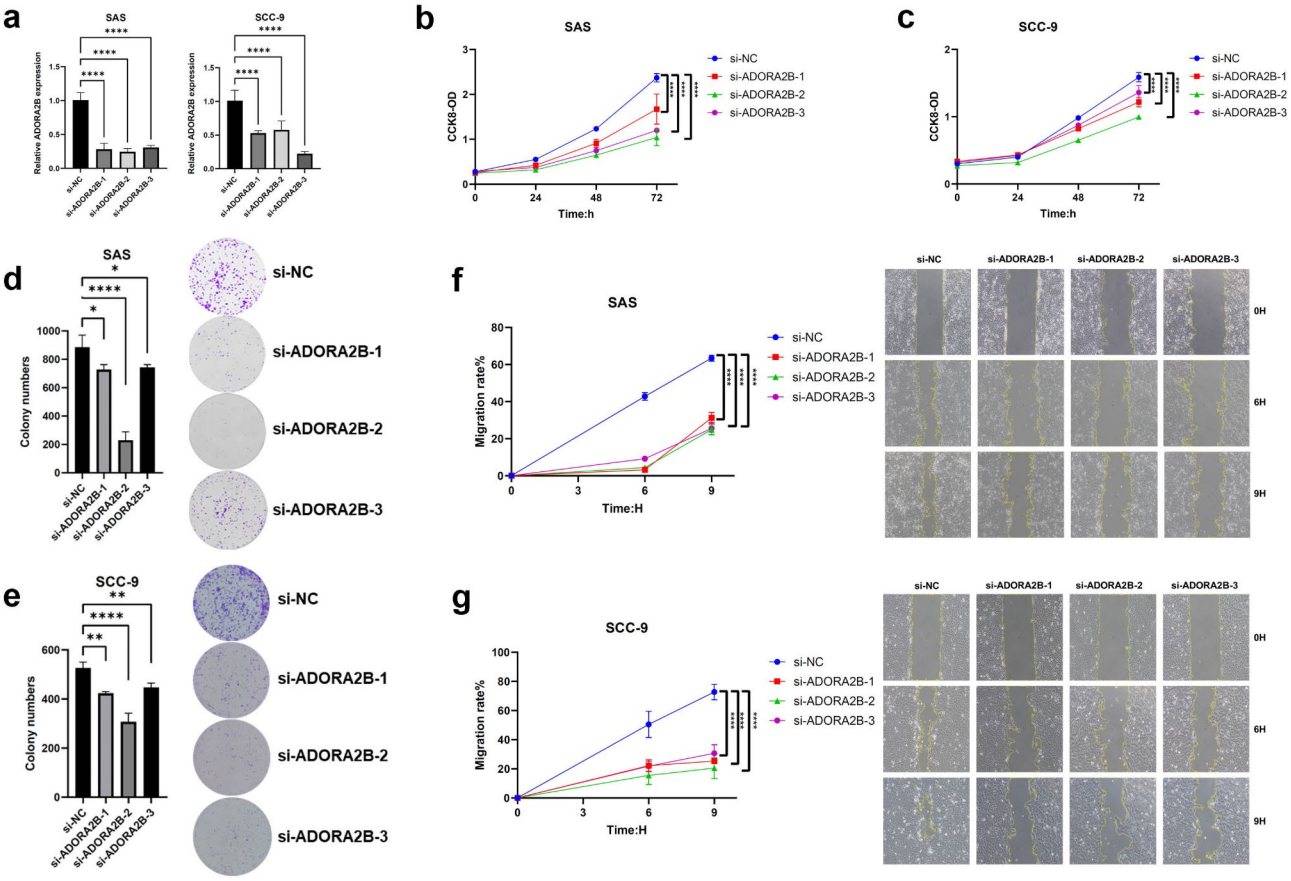

Fig. 11 Knockdown of ADORA2B inhibits the proliferation and migration of HNSC cells. QRT-PCR analysis confirming the knockdown efficiency of ADORA2B in SAS and SCC-9 cells transfected with three independent siRNAs (si-ADORA2B-1, si-ADORA2B-2, si-ADORA2B-3) compared to the negative control (si-NC) (**a**). CCK-8 assays showing reduced proliferation of SAS (**b**) and SCC-9 (**c**) cells following ADORA2B knockdown. Colony formation assays demonstrating a significant decrease in colony-forming ability in SAS (**d**) and SCC-9 (**e**) cells upon ADORA2B knockdown. Wound healing assays showing impaired migration rates in SAS (**f**) and SCC-9 (**g**) cells after ADORA2B knockdown at 0 h, 6 h, and 9 h. Abbreviations: HNSC, head and neck squamous cell carcinoma; qRT-PCR, quantitative real-time polymerase chain reaction; CCK-8, Cell Counting Kit-8. Statistical significance: *$p < 0.05$, **$p < 0.01$, ***$p < 0.001$, ****$p < 0.0001$, ns: not significant

expanded the indications for immunotherapy, providing evidence to support its integration into earlier stages of HNSC management [25–27]. This shift aims to improve long-term survival outcomes. However, a significant proportion of patients fail to benefit from immunotherapy, suggesting that the heterogeneity of the TME plays a crucial role in treatment response [28–30]. A deeper understanding of these tumor-immune interactions is essential for optimizing therapeutic strategies and extending the benefits of immunotherapy to a broader patient population.

ADORA2B is a G protein-coupled receptor that regulates inflammation, hypoxia adaptation, and immune modulation [7–9]. As a member of the adenosine receptor family, ADORA2B is primarily activated by extracellular adenosine, which is elevated under hypoxic and inflammatory conditions. Upon activation, ADORA2B primarily signals through Gs protein-mediated cyclic adenosine monophosphate accumulation, while also engaging Gq-mediated pathways, contributing to its diverse physiological effects. Beyond its role in hypoxia adaptation and inflammation, ADORA2B is implicated in cardiovascular homeostasis, ischemic injury response, and immune regulation [31–33]. Depending on the cellular and disease context, ADORA2B activation can exert both protective and pathological effects. Under ischemic and hypoxic conditions, ADORA2B promotes erythropoiesis, vascular remodeling, and tissue protection, whereas in chronic inflammatory diseases, it modulates cytokine release and immune cell function [34]. Given its widespread expression and involvement in multiple biological processes, ADORA2B has emerged as a therapeutic target in various pathological conditions. Increasingly, evidence highlights its pivotal role in tumor progression and TME modulation, particularly in promoting immune evasion and therapy resistance [7, 12, 13]. However, its precise function in HNSC remains largely unexplored.

In this study, we conducted a comprehensive analysis of ADORA2B expression in HNSC using TCGA and GEO datasets. Our findings revealed that ADORA2B is significantly overexpressed in HNSC tumor tissues compared to adjacent normal tissues, suggesting its potential as a diagnostic biomarker. Clinical correlation analysis demonstrated that higher ADORA2B expression is associated with more advanced clinical or pathological T and overall stages. Additionally, mutation analysis indicated that patients with high ADORA2B expression exhibit a higher mutation burden compared to those with lower expression levels. Survival analysis confirmed that elevated ADORA2B expression is linked to shorter OS and PFS, underscoring its prognostic significance. To further enhance prognostic prediction accuracy, we developed an ADORA2B-based nomogram. This model demonstrated superior predictive performance compared to ADORA2B expression alone, reinforcing its potential clinical utility in HNSC outcome prediction. Notably, these findings align with previous reports in ovarian, gastric, pancreatic, and lung cancers, where ADORA2B overexpression correlates with poor prognosis, advanced tumor stage, and increased metastatic potential [10, 11, 13, 35]. These parallels suggest that ADORA2B may function as a common oncogenic driver across multiple malignancies, emphasizing the need for further research into its mechanistic role in HNSC progression and therapy resistance.

ADORA2B plays a multifaceted role in tumor biology, contributing to tumor proliferation, metastasis, therapy resistance, and immune evasion through a complex interplay of intracellular signaling pathways and TME modulation [14, 35]. ADORA2B has been shown to promote tumor growth and angiogenesis by activating cell cycle regulators and anti-apoptotic pathways [14]. In lung and pancreatic cancer models, ADORA2B silencing induces G1 phase cell cycle arrest and triggers caspase-dependent apoptosis, leading to tumor growth suppression [35]. Additionally, ADORA2B-mediated vascular endothelial growth factor upregulation enhances tumor vascularization, supporting tumor expansion [14]. ADORA2B has also been implicated in tumor metastasis and epithelial-mesenchymal transition (EMT). In gastric cancer, ADORA2B overexpression correlates with lymph node metastasis, primarily via activation of the TGF-β/MAPK pathway, which drives EMT progression [11]. Similarly, in lung cancer, ADORA2B promotes cytoskeletal remodeling and cell motility through interactions with CB2 and GPR55 receptors, facilitating tumor invasion and dissemination [36]. In addition to tumor progression, ADORA2B contributes to therapy resistance, particularly in radiotherapy and chemotherapy. In glioblastoma, ADORA2B cooperates with CD73 to activate the Akt/ERK pathway, enhancing DNA damage repair and radiation resistance [37]. ADORA2B inhibition has been shown to increase cisplatin sensitivity in gastric cancer cells, likely by reversing EMT-associated drug resistance [11]. Furthermore, ADORA2B interacts with multiple oncogenic signaling pathways, reinforcing its role in tumor progression. For example, it regulates PI3K/Akt signaling to influence tumor metabolism and ferroptosis sensitivity, and activates the MAPK pathway to promote tumor-associated fibroblast differentiation and stromal remodeling [38]. Additionally, ADORA2B forms a positive feedback loop with HIF-1α, promoting angiogenesis and tumor adaptation to hypoxia [39].

To investigate the mechanisms underlying the prognostic differences between HNSC patients with high and low ADORA2B expression, we analyzed biological process differences using WGCNA. The results of functional enrichment analysis revealed notable enrichment of immune-related pathways. Specifically, hallmark pathway such as allograft rejection, inflammatory response, interferon-gamma response, complement, IL2-STAT5 signaling, and IL6-JAK-STAT3 signaling pathway were significantly downregulated in the high ADORA2B expression group. This downregulation highlights the potential immunosuppressive impact of elevated ADORA2B expression, which may compromise anti-tumor immunity in HNSC. Therefore, we further examined immune infiltration and the tumor immune microenvironment in HNSC. Consistent with expectations, HNSC patients with high ADORA2B expression showed significantly lower immune, stromal, and ESTIMATE scores. Patients with high ADORA2B expression also exhibited significantly reduced scores for most immune cell populations compared to those with low expression. These results strongly suggest that elevated ADORA2B expression is associated with a more immunosuppressive TME and impaired immune status in HNSC patients.

To explore the mechanisms underlying the prognostic disparity between HNSC patients with high and low ADORA2B expression, we performed functional enrichment analysis using WGCNA. The results revealed a notable enrichment of immune-related pathways, with several hallmark pathways, including allograft rejection, inflammatory response, interferon-gamma response, complement activation, IL2-STAT5 signaling, and IL6-JAK-STAT3 signaling, being significantly downregulated in the high ADORA2B expression group. This suppression of immune-associated pathways further underscores the immunosuppressive role of ADORA2B, which may facilitate tumor progression by evading immune surveillance. To further investigate this immunosuppressive effect, we examined immune infiltration and the TME in HNSC. As expected, patients with high ADORA2B expression exhibited markedly lower immune, stromal,

and ESTIMATE scores, indicating a more immunosuppressive TME. Additionally, infiltration levels of the majority of immune cell populations were significantly decreased in the high ADORA2B expression group compared to those with low expression. Collectively, these findings suggest that ADORA2B may contribute to poor prognosis in HNSC by impairing anti-tumor immune responses and promoting an immunosuppressive microenvironment.

Furthermore, we explored the relationship between ADORA2B expression and immunotherapy response, particularly in the context of ICB therapy. Our analysis revealed that patients with low ADORA2B expression who underwent ICB treatment exhibited significantly improved survival outcomes compared to those with high expression levels. Moreover, patients who responded favorably to ICB therapy (complete or partial response) had notably lower ADORA2B expression than those with stable or progressive disease. These findings indicate that ADORA2B expression levels may serve as a predictive biomarker for ICB efficacy, where high ADORA2B expression identifies tumors with potential resistance to immunotherapy.

Emerging evidence highlights the role of adenosine receptor signaling in tumor immune evasion and resistance to immunotherapy. In pancreatic cancer, ADORA2B activation enhances immunosuppression, promoting tumor progression and reducing immunotherapy efficacy [40]. Additionally, hypoxia-induced adenosine accumulation further amplifies ADORA2B-mediated immune suppression by modulating multiple immune cell types, including T cells, macrophages, and dendritic cells, ultimately impairing adaptive anti-tumor responses [7]. Notably, ADORA1 inhibition has been shown to upregulate PD-L1 expression via ATF3, leading to immune escape and reduced anti-tumor immunity in melanoma and non-small cell lung cancer [41]. Given our findings that high ADORA2B expression correlates with reduced immune infiltration and poor response to ICB therapy, it is plausible that ADORA2B contributes to immune resistance through similar mechanisms. Targeting ADORA2B may help restore anti-tumor immunity and enhance ICB efficacy in HNSC, warranting further investigation into its role in immune checkpoint regulation and therapy resistance.

To identify potential therapeutic strategies for patients with high ADORA2B expression, we conducted a correlation analysis between ADORA2B expression and drug sensitivity. The results identified several candidate agents, including Ixazomib citrate, Homoharringtonine, Masitinib, Pevonedistat, Amuvatinib, Arsenic trioxide, Parthenolide, and Imetelstat, which exhibited a negative correlation with ADORA2B expression, suggesting that tumors with high ADORA2B expression may be more responsive to these drugs. Among these candidate drugs, Homoharringtonine and Arsenic trioxide have already been applied in the field of cancer treatment to some extent, and relevant research progress provides important references for their potential applications in patients with high ADORA2B expression. Specifically, Homoharringtonine, a natural alkaloid, has demonstrated significant pharmacological potential in the treatment of hematologic malignancies in recent years, with its multifaceted mechanisms of action contributing to therapeutic outcomes [42, 43]. It can induce apoptosis, inhibit cell cycle progression, and reduce cell migration and invasion. Notably, Homoharringtonine has exhibited potent antitumor effects in various hematologic malignancies, such as acute myeloid leukemia and chronic myeloid leukemia, thereby underscoring its clinical relevance [42]. Additionally, Homoharringtonine has been found to inhibit the NOTCH/MYC signaling pathway, significantly prolonging survival in both in vivo and in vitro models of T-cell acute lymphoblastic leukemia [43]. Arsenic trioxide is also a widely used drug in cancer treatment, particularly demonstrating remarkable efficacy in treating acute promyelocytic leukemia, where it has become a first-line therapeutic agent [44, 45]. Arsenic trioxide can induce apoptosis in various cancer cells, primarily through the regulation of multiple signaling pathways. For example, in prostate cancer research, Arsenic trioxide in combination with curcumin exerts synergistic anticancer effects by targeting specific signaling pathways [46]. In non-hematologic malignancies, Arsenic trioxide has also demonstrated certain antitumor potential, as evidenced by pancreatic cancer research, which has explored its molecular and epigenetic mechanisms in combination therapies [47]. In summary, as drugs with an established foundation in cancer treatment, Homoharringtonine and Arsenic trioxide warrant further investigation for their potential applications in HNSC patients with high ADORA2B expression. Future research should focus on elucidating the specific molecular mechanisms underlying the interactions between these two drugs and ADORA2B, as well as evaluating their efficacy and safety in tumor models with high ADORA2B expression, thereby providing stronger scientific evidence for the development of personalized treatment strategies for HNSC patients with high ADORA2B expression.

To further validate the functional role of ADORA2B in HNSC, we performed cytological experiments to assess its impact on cell proliferation and migration. CCK-8 assays demonstrated that ADORA2B knockdown significantly inhibited HNSC cell proliferation. Similarly, colony formation assays revealed that silencing ADORA2B led to a marked reduction in colony-forming ability. Moreover, wound healing assays showed that ADORA2B knockdown significantly impaired the migratory capacity of HNSC cells, further supporting its role in tumor

cell motility. Taken together, these experimental results strongly support the view that ADORA2B actively drives HNSC cell proliferation and migration, and highlight its potential as a therapeutic target for intervention.

Despite these findings, our study has several limitations. First, as a retrospective analysis, it is inherently subject to selection bias, necessitating prospective validation in independent cohorts to confirm these observations. Additionally, while we demonstrated the impact of ADORA2B on HNSC cell proliferation and migration, our study did not extend to in-depth mechanistic investigations. Future studies should focus on elucidating the molecular pathways through which ADORA2B promotes tumor progression and immune modulation, utilizing both in vivo models and advanced molecular techniques.

Conclusions

This study identifies ADORA2B as a key oncogenic driver in HNSC. ADORA2B is significantly overexpressed in HNSC and correlates with advanced clinical stages, poor survival outcomes, and an immunosuppressive tumor microenvironment. Functional experiments demonstrated that ADORA2B knockdown significantly inhibits HNSC cell proliferation, colony formation, and migration, confirming its critical role in tumor progression. Moreover, the association of high ADORA2B expression with reduced immune infiltration and suppressed anti-tumor immune responses further underscores its role in shaping an immunosuppressive tumor microenvironment. Additionally, high ADORA2B expression is associated with resistance to immune checkpoint blockade therapy, highlighting its potential as a predictive biomarker for immunotherapy response. We also identified candidate therapeutic agents targeting ADORA2B, providing a foundation for personalized treatment strategies. These therapeutic agents hold promise for overcoming treatment resistance in patients with high ADORA2B expression. While these findings establish ADORA2B as a promising diagnostic, prognostic, and therapeutic target, further in vivo studies and mechanistic investigations are required to fully elucidate its role in HNSC progression and therapy resistance. Future research should also focus on validating these therapeutic strategies in clinical settings to optimize treatment outcomes for HNSC patients.

Abbreviations

ADORA2B	Adenosine a2b receptor
HNSC	Head and neck squamous cell carcinoma
TCGA	The cancer genome atlas
GEO	Gene expression omnibus
WGCNA	Weighted gene co-expression network analysis
ssGSEA	single-sample gene set enrichment analysis
ICB	Immune checkpoint blockade
OS	Overall survival
PFS	Progression-free survival
TME	Tumor microenvironment
GO	Gene ontology
ROC	Receiver operating characteristic
AUC	Area under the curve
TMB	Tumor mutation burden
C-index	Concordance index
CESC	Cervical squamous cell carcinoma and endocervical adenocarcinoma
CHOL	Cholangiocarcinoma
ESCA	Esophageal carcinoma
KIRC	Kidney renal clear cell carcinoma
LIHC	Liver hepatocellular carcinoma
LUAD	Lung adenocarcinoma
LUSC	Lung squamous cell carcinoma
PAAD	Prostate adenocarcinoma
STAD	Stomach adenocarcinoma
LGG	Lower-grade glioma
MESO	Mesothelioma
TOM	Topological overlap matrix
BP	Biological processes
CC	Cellular components
MF	Molecular function
KEGG	Kyoto encyclopedia of genes and genomes

Supplementary Information

The online version contains supplementary material available at https://doi.org/10.1186/s12885-025-14102-2.

Supplementary Material 1

Acknowledgements

We acknowledge the TCGA and GEO database for providing the platform and its contributors for uploading meaningful datasets.

Author contributions

Jun-yan He designed the research. Pian Li, Ke-ling Pang, Shuang-jing Chen, Dong Yang, Ai-tao Nai, Gui-cheng He, Zhe Fang and Qiao Yang collected and analysed the data. Man-bo Cai drafted the manuscript. Pian Li, Ke-ling Pang, Man-bo Cai and Jun-yan He prepared the figures. Man-bo Cai and Jun-yan He revised the manuscript. All the authors have read and approved the final version of the manuscript.

Funding

This work was supported by National Natural Science Foundation of China (82304083 to Jun-yan He) and Natural Science Foundation of Hunan Province (2023JJ40584 to Jun-yan He).

Data availability

The datasets analyzed in the current study are available from TCGA (https://portal.gdc.cancer.gov/) and GEO (https://www.ncbi.nlm.nih.gov/geo/).

Declarations

Ethics approval and consent to participate

Not applicable.

Consent for publication

Not applicable.

Competing interests

The authors declare no competing interests.

Author details

[1]Department of Oncology, The First Affiliated Hospital, Hengyang Medical School, University of South China, Hengyang, Hunan, China
[2]Affiliated Tumor Hospital of Guangxi Medical University, Nanning, China
[3]The PLA Rocket Force Characteristic Medical Center, Beijing, China

Received: 14 February 2025 / Accepted: 7 April 2025
Published online: 12 April 2025

References

1. Siegel RL, Giaquinto AN, Jemal A. Cancer statistics, 2024. CA Cancer J Clin. 2024;74(1):12–49.
2. Johnson DE, Burtness B, Leemans CR, Lui VWY, Bauman JE, Grandis JR. Head and neck squamous cell carcinoma. Nat Rev Dis Primers. 2020;6(1):92.
3. Plath M, Gass J, Hlevnjak M, Li Q, Feng B, Hostench XP, et al. Unraveling most abundant mutational signatures in head and neck cancer. Int J Cancer. 2021;148(1):115–27.
4. Ruffin AT, Li H, Vujanovic L, Zandberg DP, Ferris RL, Bruno TC. Improving head and neck cancer therapies by Immunomodulation of the tumour microenvironment. Nat Rev Cancer. 2023;23(3):173–88.
5. Bhatia A, Burtness B. Treating head and neck cancer in the age of immunotherapy: A 2023 update. Drugs. 2023;83(3):217–48.
6. Orland MD, Ullah F, Yilmaz E, Geiger JL. Immunotherapy for head and neck squamous cell carcinoma: present and future approaches and challenges. JCO Oncol Pract. 2024;20(12):1588–95.
7. Strickland LN, Faraoni EY, Ruan W, Yuan X, Eltzschig HK, Bailey-Lundberg JM. The resurgence of the Adora2b receptor as an immunotherapeutic target in pancreatic cancer. Front Immunol. 2023;14:1163585.
8. Cabalín C, Villalobos-Labra R, Toledo F, Sobrevia L. Involvement of A(2B) adenosine receptors as anti-inflammatory in gestational diabesity. Mol Aspects Med. 2019;66:31–9.
9. Eltzschig HK, Bonney SK, Eckle T. Attenuating myocardial ischemia by targeting A2B adenosine receptors. Trends Mol Med. 2013;19(6):345–54.
10. Chi L, Huan L, Zhang C, Wang H, Lu J. Adenosine receptor A2b confers ovarian cancer survival and PARP inhibitor resistance through IL-6-STAT3 signalling. J Cell Mol Med. 2023;27(15):2150–64.
11. Wang H, Tan F, Xu Y, Ma Y, Li Y, Xiao H. Adenosine receptor A2B antagonist inhibits the metastasis of gastric cancer cells and enhances the efficacy of cisplatin. Technol Cancer Res Treat. 2023;22:15330338221150318.
12. Kasama H, Sakamoto Y, Kasamatsu A, Okamoto A, Koyama T, Minakawa Y, et al. Adenosine A2b receptor promotes progression of human oral cancer. BMC Cancer. 2015;15:563.
13. Faraoni EY, Singh K, Chandra V, Le Roux O, Dai Y, Sahin I, et al. CD73-Dependent adenosine signaling through Adora2b drives immunosuppression in ductal pancreatic cancer. Cancer Res. 2023;83(7):1111–27.
14. Wilkat M, Bast H, Drees R, Dünser J, Mahr A, Azoitei N, et al. Adenosine receptor 2B activity promotes autonomous growth, migration as well as vascularization of head and neck squamous cell carcinoma cells. Int J Cancer. 2020;147(1):202–17.
15. Liao C, Wang X. TCGAplot: an R package for integrative pan-cancer analysis and visualization of TCGA multi-omics data. BMC Bioinformatics. 2023;24(1):483.
16. Robin X, Turck N, Hainard A, Tiberti N, Lisacek F, Sanchez JC, et al. pROC: an open-source package for R and S + to analyze and compare ROC curves. BMC Bioinformatics. 2011;12:77.
17. Mayakonda A, Lin DC, Assenov Y, Plass C, Koeffler HP. Maftools: efficient and comprehensive analysis of somatic variants in cancer. Genome Res. 2018;28(11):1747–56.
18. ForestPlots.net, Blundo C, Carilla J, Grau R, Malizia A, Malizia L, et al. Taking the pulse of Earth's tropical forests using networks of highly distributed plots. Biol Conserv. 2021;260:108849.
19. Blanche P, Dartigues JF, Jacqmin-Gadda H. Estimating and comparing time-dependent areas under receiver operating characteristic curves for censored event times with competing risks. Stat Med. 2013;32(30):5381–97.
20. Langfelder P, Horvath S. WGCNA: an R package for weighted correlation network analysis. BMC Bioinformatics. 2008;9:559.
21. Yu G, Wang LG, Han Y, He QY. ClusterProfiler: an R package for comparing biological themes among gene clusters. Omics. 2012;16(5):284–7.
22. Yoshihara K, Shahmoradgoli M, Martínez E, Vegesna R, Kim H, Torres-Garcia W, et al. Inferring tumour purity and stromal and immune cell admixture from expression data. Nat Commun. 2013;4:2612.
23. Hänzelmann S, Castelo R, Guinney J. GSVA: gene set variation analysis for microarray and RNA-seq data. BMC Bioinformatics. 2013;14:7.
24. Jiang C, Wang S, Zhu L. Efficacy and safety of immunotherapy for head and neck squamous cell carcinoma: a meta-analysis of randomized clinical trials. Front Oncol. 2024;14:1489451.
25. Nederlof I, Isaeva OI, de Graaf M, Gielen R, Bakker NAM, Rolfes AL, et al. Neoadjuvant nivolumab or nivolumab plus ipilimumab in early-stage triple-negative breast cancer: a phase 2 adaptive trial. Nat Med. 2024;30(11):3223–35.
26. Li K, Chen J, Hu Y, Wang YZ, Shen Y, Chen G, et al. Neoadjuvant chemotherapy plus camrelizumab for locally advanced cervical cancer (NACI study): a multicentre, single-arm, phase 2 trial. Lancet Oncol. 2024;25(1):76–85.
27. Chen X, Xu X, Wang D, Liu J, Sun J, Lu M et al. Neoadjuvant sintilimab and chemotherapy in patients with potentially resectable esophageal squamous cell carcinoma (KEEP-G 03): an open-label, single-arm, phase 2 trial. J Immunother Cancer. 2023;11(2).
28. Zhang YJ, Xiao Y, Li ZZ, Bu LL. Immunometabolism in head and neck squamous cell carcinoma: hope and challenge. Biochim Biophys Acta Mol Basis Dis. 2024;1871(3):167629.
29. Lee AM, Weaver AN, Acosta P, Harris L, Bowles DW. Review of current and future medical treatments in head and neck squamous cell carcinoma. Cancers (Basel). 2024;16(20).
30. Okuyama K, Naruse T, Yanamoto S. Tumor microenvironmental modification by the current target therapy for head and neck squamous cell carcinoma. J Exp Clin Cancer Res. 2023;42(1):114.
31. Ruan W, Li J, Choi S, Ma X, Liang Y, Nair R et al. Targeting myocardial equilibrative nucleoside transporter ENT1 provides cardioprotection by enhancing myeloid Adora2b signaling. JCI Insight. 2023;8(11).
32. Lim B, Jung K, Gwon Y, Oh JG, Roh JI, Hong SH, et al. Cardioprotective role of APIP in myocardial infarction through ADORA2B. Cell Death Dis. 2019;10(7):511.
33. Dietz S, Hebel J, Rühle J, Huff A, Eltzschig HK, Lajqi T, et al. Impact of the adenosine receptor A2BR expressed on myeloid cells on immune regulation during pregnancy. Eur J Immunol. 2024;54(12):e2451149.
34. Li X, Berg NK, Mills T, Zhang K, Eltzschig HK, Yuan X. Adenosine at the interphase of hypoxia and inflammation in lung injury. Front Immunol. 2020;11:604944.
35. Sui Y, Liu J, Zhang J, Zheng Z, Wang Z, Jia Z, et al. Expression and gene regulation network of adenosine receptor A2B in lung adenocarcinoma: A potential diagnostic and prognostic biomarker. Front Mol Biosci. 2021;8:663011.
36. Oyama M, Sakamoto M, Kitabatake K, Shiina K, Kitahara D, Onozawa S, et al. Involvement of cannabinoid receptors and adenosine A2B receptor in enhanced migration of lung cancer A549 cells induced by γ-Ray irradiation. Biol Pharm Bull. 2024;47(1):60–71.
37. Kitabatake K, Kaji T, Tsukimoto M. Involvement of CD73 and A2B receptor in Radiation-Induced DNA damage response and cell migration in human glioblastoma A172 cells. Biol Pharm Bull. 2021;44(2):197–210.
38. Li S, Han J, Cao J, Han H, Lu B, Wen T, et al. ADORA2B, transcriptionally suppressing by MYC, promotes ferroptosis of chondrocytes via Inhibition of the PI3K/Akt pathway in mice with osteoarthritis. Environ Toxicol. 2024;39(5):2487–501.
39. Iriyama T, Wang W, Parchim NF, Sayama S, Kumasawa K, Nagamatsu T, et al. Reciprocal upregulation of hypoxia-inducible factor-1α and persistently enhanced placental adenosine signaling contribute to the pathogenesis of preeclampsia. Faseb J. 2020;34(3):4041–54.
40. DelGiorno K. CD73 is a critical immune checkpoint in a molecular subtype of pancreatic cancer. Cancer Res. 2023;83(7):977–8.
41. Liu H, Kuang X, Zhang Y, Ye Y, Li J, Liang L, et al. ADORA1 Inhibition promotes tumor immune evasion by regulating the ATF3-PD-L1 axis. Cancer Cell. 2020;37(3):324–e398.
42. Suo S, Zhao D, Li F, Zhang Y, Rodriguez-Rodriguez S, Nguyen LXT, et al. Homoharringtonine inhibits the NOTCH/MYC pathway and exhibits antitumor effects in T-cell acute lymphoblastic leukemia. Blood. 2024;144(12):1343–7.
43. Yan M, Wang H, Wei R, Li W. Arsenic trioxide: applications, mechanisms of action, toxicity and rescue strategies to date. Arch Pharm Res. 2024;47(3):249–71.
44. Jiang Y, Shen X, Zhi F, Wen Z, Gao Y, Xu J, et al. An overview of arsenic trioxide-involved combined treatment algorithms for leukemia: basic concepts and clinical implications. Cell Death Discov. 2023;9(1):266.
45. Mirzaei A, Jahanshahi F, Khatami F, Reis LO, Aghamir SMK. Human prostate cancer cell epithelial-to-mesenchymal transition as a novel target of arsenic trioxide and Curcumin therapeutic approach. Tissue Cell. 2022;76:101805.
46. Sarwar A, Zhu Z, Zhu M, Tang X, Su Q, Yang T, et al. Homoharringtonine sensitizes pancreatic cancer to erlotinib by direct targeting and miRNA-130b-3p-mediated EphB4-JAK2-STAT3 axis. J Pharm Pharmacol. 2023;75(10):1294–309.
47. Wang W, He L, Lin T, Xiang F, Wu Y, Zhou F, et al. Homoharringtonine: mechanisms, clinical applications and research progress. Front Oncol. 2025;15:1522273.

Publisher's note